A&A 535, A29 (2011)
DOI: 10.1051/0004-6361/201117746

Astronomy & Astrophysics

Search for OB stars running away from young star clusters

II. The NGC 6357 star-forming region

V. V. Gvaramadze[1,2,3], A. Y. Kniazev[4,5], P. Kroupa[1], and S. Oh[1]

[1] Argelander-Institut für Astronomie, Universität Bonn, Auf dem Hügel 71, 53121 Bonn, Germany
e-mail: [pavel;skoh]@astro.uni-bonn.de
[2] Sternberg Astronomical Institute, Moscow State University, Universitetskij Pr. 13, Moscow 119992, Russia
e-mail: vgvaram@mx.iki.rssi.ru
[3] Isaac Newton Institute of Chile, Moscow Branch, Universitetskij Pr. 13, Moscow 119992, Russia
[4] South African Astronomical Observatory, PO Box 9, 7935 Observatory, Cape Town, South Africa
e-mail: akniazev@saao.ac.za
[5] Southern African Large Telescope Foundation, PO Box 9, 7935 Observatory, Cape Town, South Africa

Received 21 July 2011 / Accepted 7 September 2011

ABSTRACT

Dynamical few-body encounters in the dense cores of young massive star clusters are responsible for the loss of a significant fraction of their massive stellar content. Some of the escaping (runaway) stars move through the ambient medium supersonically and can be revealed via detection of their bow shocks (visible in the infrared, optical or radio). In this paper, which is the second of a series of papers devoted to the search for OB stars running away from young ($\lesssim$ several Myr) Galactic clusters and OB associations, we present the results of the search for bow shocks around the star-forming region NGC 6357. Using the archival data of the Midcourse Space Experiment (MSX) satellite and the *Spitzer* Space Telescope, and the preliminary data release of the Wide-Field Infrared Survey Explorer (WISE), we discovered seven bow shocks, whose geometry is consistent with the possibility that they are generated by stars expelled from the young (~1–2 Myr) star clusters, Pismis 24 and AH03 J1725-34.4, associated with NGC 6357. Two of the seven bow shocks are driven by the already known OB stars, HD 319881 and [N78] 34. Follow-up spectroscopy of three other bow-shock-producing stars showed that they are massive (O-type) stars as well, while the 2MASS photometry of the remaining two stars suggests that they could be B0 V stars, provided that both are located at the same distance as NGC 6357. Detection of numerous massive stars ejected from the very young clusters is consistent with the theoretical expectation that star clusters can effectively lose massive stars at the very beginning of their dynamical evolution (long before the second mechanism for production of runaway stars, based on a supernova explosion in a massive tight binary system, begins to operate) and lends strong support to the idea that probably all field OB stars have been dynamically ejected from their birth clusters. A by-product of our search for bow shocks around NGC 6357 is the detection of three circular shells typical of luminous blue variable and late WN-type Wolf-Rayet stars.

Key words. stars: kinematics and dynamics – stars: massive – open clusters and associations: general – open clusters and associations: individual: AH03 J1725−34.4 – ISM: individual objects: NGC 6357

1. Introduction

Close few-body dynamical encounters in the dense cores of young massive star clusters are responsible for the loss of a significant fraction of OB stars at the early stages of cluster evolution (Poveda et al. 1967; Aarseth & Hills 1972; Gies 1987; Leonard & Duncan 1990; Kroupa 2004; Pflamm-Altenburg & Kroupa 2006; Moeckel & Bate 2010). The high central densities in young clusters (the necessary condition for the production of runaway stars) could be either primordial (e.g. Clarke & Pringle 1992; Murray & Lin 1996; Clarke & Bonnell 2008) or caused by dynamical mass segregation (e.g. Portegies Zwart et al. 1999; Gürkan et al. 2004; Allison et al. 2009). In both cases, the clusters start to eject stars long before the most massive cluster members explode in supernovae, i.e. long before the binary-supernova ejection mechanism (Blaauw 1961) begins to operate. Moreover, runaway stars could leave their parent clusters already during the cluster formation process if a core of massive protostars forms before bulk gas expulsion from the embedded cluster.

The runaway OB stars can be revealed either directly, via measurement of their proper motions and/or radial velocities (e.g. Moffat et al. 1998; Mdzinarishvili & Chargeishvili 2005; Massey et al. 2005; Evans et al. 2010; Tetzlaff, Neuhäuser & Hohle 2011), or indirectly, through the detection of bow shocks around them (Gvaramadze & Bomans 2008b; Gvaramadze et al. 2010a; Gvaramadze, Kroupa & Pflamm-Altenburg 2010d; Gvaramadze, Pflamm-Altenburg & Kroupa 2011a; Gvaramadze et al. 2011b). The latter possibility is especially helpful for those runaways whose proper motions are still not available or are measured with a low significance. The geometry of detected bow shocks can be used to infer the direction of the stellar motion and thereby to determine possible parent clusters for the bow-shock-producing field stars (Gvaramadze & Bomans 2008b; Gvaramadze et al. 2010a,d, 2011a).

The present paper is the second of a series of papers devoted to the search for OB stars running away from young ($\lesssim$several Myr) Galactic clusters and OB associations. In Gvaramadze & Bomans (2008b; hereafter Paper I), we reported the detection of three bow shocks produced by OB stars running away from the star cluster NGC 6611. Now we report the discovery of seven bow shocks within ~1°.5 from the star-forming region NGC 6357 and its associated (massive) star clusters Pismis 24

and AH03 J1725−34.4. The geometry of all seven bow shocks suggests that they are driven by stars expelled from NGC 6357. In Sect. 2 we review the relevant data for the star clusters associated with NGC 6357. Section 3 presents the results of the search for bow shocks around NGC 6357. The bow-shock-producing stars are identified and discussed in Sect. 4. In Sect. 5 we present the discovery of three circular shells around NGC 6357. Section 6 deals with questions related to the content of the paper. We summarize in Sect. 7.

2. Star-forming region NGC 6357 and its associated star clusters

NGC 6357 is an extended (~40′ × 60′ or ~20 pc × 30 pc at a distance of 1.7 kpc; see below) H II region of ongoing massive star-formation in the Sagittarius arm. At radio wavelengths NGC 6357 is dominated by the two components G 353.2+0.9 and G 353.1+0.6 (Schraml & Mezger 1969; Felli et al. 1990). Two open star clusters, Pismis 24 and AH03 J1725−34.4, are associated with these components, respectively. The first cluster was extensively studied during the last years, while only sparse information exists on the second one. Below we review the observational data on both clusters in turn.

2.1. Pismis 24

Pismis 24 was recognized as an open star cluster by Pismis (1959). It is believed that the massive stars of this cluster are the main ionizing source responsible for the origin of the H II region NGC 6357 (Lortet et al. 1984; Bohigas et al. 2004; Cappa et al. 2011). Line observations of a molecular cloud associated with NGC 6357 showed that most of the molecular emission arises from the regions behind or to the north of Pismis 24, which indicates that the cluster is immersed in a blister-like H II region viewed face-on (Massi et al. 1997).

The cluster contains two very massive O3.5-type stars (Massey, DeGioia-Eastwood & Waterhouse 2001; Walborn et al. 2002), one of which, Pismis 24-1, was believed to be one of the most massive known stars in the Galaxy, with an inferred mass larger than 200 $M_{\odot}$ (Walborn et al. 2002). Subsequent *Hubble* Space Telescope observations resolved Pismis 24-1 into two visual components, while follow-up spectroscopy showed that one of the components (Pismis 24-1SW) is an O4 III(f+) star (of mass of ~100 $M_{\odot}$) and the second one (Pismis 24-1NE) is a very massive (~100 $M_{\odot}$) short-period spectroscopic binary (Maíz Apellániz et al. 2007).

Because of the high visual extinction towards Pismis 24 (≃5–15 mag; Wang et al. 2007), the stellar content of the cluster was poorly studied until recently, so that only the most luminous and less reddened cluster members (about two dozen altogether) were identified, either by means of photometry or spectroscopy (Moffat & Vogt 1973; Neckel 1978, 1984; Lortet et al. 1984; Massey et al. 2001). One of these stars is a binary system (HD 157504) composed of a WC7 Wolf-Rayet star (WR 93) and an O7-9 star (van der Hucht 2001).

Thanks to the ability of X-ray observations to penetrate heavy absorption, the situation was improved with *Chandra*/ACIS observations of NGC 6357, which allowed the detection of even the low-mass pre-main-sequence population of Pismis 24 (with masses extending down to ~0.3 $M_{\odot}$), thereby increasing the number of the cluster members by a factor of ~50 and bringing it to ≃10 000 (Wang et al. 2007). Most of these stars are concentrated in a compact core of angular radius of ≃2 arcmin (or ≃1.0 pc), which is centred on the two most massive stars in the cluster, Pismis 24-1 and Pismis 24-17[1], while the remaining stars are spread with an approximately exponential distribution over a halo of radius of ≃11 arcmin (≃5.4 pc). The *Chandra* observation also detected two dozens of X-ray sources, whose luminosities and colours suggest that they could be OB stars. If spectroscopic follow-ups of these stars will prove that they are indeed massive, then the OB star content of Pismis 24 will be doubled. Assuming that *Chandra* detected all stars with mass >0.3 $M_{\odot}$ and using the Kroupa (2001) IMF (which is a two-part power-law IMF with a slope $\alpha_1 = 1.3$ for stellar masses between 0.08 and 0.5 $M_{\odot}$, and a Salpeter slope $\alpha_2 = 2.3$ for more massive stars), one finds a mass of the cluster of ~10^4 $M_{\odot}$ and the expected number of OB stars in the cluster of ~100. The latter figure exceeds the number of confirmed and candidate OB stars (i.e. 44 stars; Wang et al. 2007) by a factor of 2, from which one can conclude that either the IMF of the cluster's members is steeper than the Salpeter one or most OB stars were already ejected from the cluster (cf. Paper I; Pflamm-Altenburg & Kroupa 2006; Moeckel & Bate 2010)[2]. In the latter case, one can expect to find numerous OB stars all around the cluster (see Sect. 3).

The simultaneous presence in Pismis 24 of several very young (~1 Myr) and very massive (≃90−100 $M_{\odot}$) stars (Maíz Apellániz et al. 2007) and the more evolved (≳2−2.5 Myr old) WC7 star WR 93 (Massey et al. 2001) leads to an age discrepancy. To overcome this discrepancy, one can assume that the star-formation process in the cluster was not coeval or that WR 93 is projected by chance near the line of sight to the cluster (note that WR 93 is located only 4 arcmin away from the cluster centre, i.e. well within the cluster halo). In the latter case it is plausible that the parent cluster of WR 93 is associated with the same molecular cloud as Pismis 24 but is totally obscured by the dusty material of the cloud, while the star itself is observable only because it is a runaway, which already escaped from the densest part of the cloud (cf. Gvaramadze et al. 2010a). Note that the coexistence of evolved and very young massive stars in the same star-forming region is not a rare occurrence. For example, two evolved (~4 Myr old) massive stars are projected against the young (≃1 Myr) very massive cluster NGC 3603, one of which, the blue supergiant star Sher 25, is separated from the cluster core by less than 20 arcsec (or 1 pc in projection; e.g. Melena et al. 2008; Rochau et al. 2010). Another possible explanation for the age discrepancy is that the most massive stars in the cluster are blue stragglers, formed because of merging of less massive stars in the course of close dynamical encounters in the cluster's core (cf. Gvaramadze & Bomans 2008a; Paper I).

Numerous distance estimates for Pismis 24 range from ≃1.7 to 2.6 kpc (e.g. Moffat & Vogt 1973; Neckel 1978, 1984; Lortet et al. 1984; Massey et al. 2001), putting the cluster in the Sagittarius spiral arm. To constrain the distance to Pismis 24, we used the optical (Massey et al. 2001) and near-infrared (2MASS; Skrutskie et al. 2006) photometry of all (six) known dwarf O stars in the cluster (see Table 2 in Massey et al. 2001) and the

[1] Note that the coordinates of Pismis 24 given in the SIMBAD database are significantly (~16 arcmin) off the position of these stars and rather correspond to the second star cluster, AH03 J1725−34.4, associated with NGC 6357. The latter cluster is confused with Pismis 24 in the WEBDA database (`http://www.univie.ac.at/webda/`) as well.

[2] The discrepancy between the "observed" and expected number of OB stars in Pismis 24 would be less severe if most massive stars residing in the cluster are binaries with mass ratio close to unity (cf. Clarke & Pringle 1992).

UBVJHK synthetic photometry of Galactic O stars by Martins & Plez (2006). Assuming that the standard total-to-selective absorption ratio $R_V = A_V/E(B-V) = 3.1$ is valid for Pismis 24 and using the optical photometry, one finds a true distance modulus of ≃12.0 mag and a distance of 2.5 kpc, which agree well with those derived by Massey et al. (2001) on the basis of a different calibration of stellar parameters. On the other hand, adopting the extinction law from Rieke & Rebofsky (1985), so that

$$A_{K_s} = 0.66E(J - K_s), \quad (1)$$

and using the 2MASS photometry, one finds a true distance modulus of ≃11.15 mag and a distance of 1.7 kpc. The discrepancy between the two distance estimates could be understood if the reddening towards Pismis 24 is anomalous, i.e. $R_V > 3.1$. One can show that $R_V \simeq 3.6$ would be enough to reconcile the distance estimates (cf. with Neckel & Chini 1981, who found $R_V = 3.8$ for NGC 6357). The distance of 1.7 kpc could also be derived if one estimates the visual extinction A_V using the relationship

$$A_V = 1.39E(V - J), \quad (2)$$

which, according to Tapia et al. (1988), is valid across the Galaxy, irrespective of high R_V values (see also Persi & Tapia 2008). This distance is consistent with that to the H II region NGC 6334 (≃1.7 kpc; Persi & Tapia 2008), located on the sky at ∼2° to the southwest from NGC 6357. It is believed that both these H II regions form a single high-mass star-forming complex (Russeil et al. 2010 and references therein). In the following we adopt a distance of 1.7 kpc for Pismis 24 (and the star-forming region NGC 6357 as a whole) so that 1° corresponds to ≃30 pc.

2.2. AH03 J1725−34.4

The second cluster, AH03 J1725−34.4, embedded in the star-forming region NGC 6357, is located at ≃0.°26 (or ≃7.5 pc in projection) to the southeast from Pismis 24 (Dias et al. 2002). The available information on this cluster is very scarce. AH03 J1725−34.4 contains at least four OB stars (Neckel 1984; Damke et al. 2006). Two of them, [N78] 49 and [N78] 51, are very massive ones, with spectral types (O4 III((f*)) and O3.5 V, respectively; Damke et al. 2006) comparable to those of the most massive stars in Pismis 24. Unfortunately, AH03 J1725−34.4 was not covered by the *Chandra* observations of NGC 6357, so that the actual extent and the stellar content of the cluster are still unknown. The presence of two very massive stars in the cluster, however, suggests that it should be as young (∼1−2 Myr) and at least half as massive as Pismis 24.

3. Search for bow shocks

A rich massive stellar content of Pismis 24 and the presence of very massive (binary) stars in both clusters associated with NGC 6357 suggest that this star-forming region was very efficient in producing runaway stars (e.g. Gvaramadze 2007; Gvaramadze et al. 2009a; Gvaramadze & Gualandris 2011). One can, therefore, expect to find some of the runaways via detection of their associated bow shocks – the natural attributes of supersonically moving stars (Baranov et al. 1971; Weaver et al. 1977). The characteristic scale of a bow shock, l, depends on the number density of the ambient medium, n, on the stellar mass-loss rate, $\dot{M}$, and on the stellar space velocity, v_*, as follows: $l \propto n^{-1/2}$, $l \propto \dot{M}^{1/2}$ and $l \propto v_*^{-1}$ (Baranov et al. 1971). The bow shocks are usually most prominent in the mid-infrared (e.g. van Buren & McCray 1988; van Buren et al. 1995; Paper I; Gvaramadze et al. 2010d,b), but can also be detected in the optical (e.g. Kaper et al. 1997; Brown & Bomans 2005; Paper I) and radio (Benaglia et al. 2010) wavebands. It should be noted that only a minority (≃20 per cent) of runaway OB stars are associated with (detectable) bow shocks (van Buren 1993; van Buren et al. 1995; Huthoff & Kaper 2002; Gvaramadze et al. 2010d). The paucity of the bow-shock-producing stars is mostly due to the fact that the majority of runaway stars are moving through a low-density, hot medium, so that the emission measure of their bow shocks is below the detection limit or the bow shocks cannot be formed at all because the sound speed in the local interstellar medium is higher than the stellar space velocity (Kaper et al. 1999; Huthoff & Kaper 2002). Moreover, the bow shocks generated by runaway stars receding from NGC 6357 and interacting with the dense material of the background (parent) molecular cloud (see Sect. 2) would be very compact and therefore hardly detectable, while those projected against the H II region might be hidden by its bright emission (see Fig. 1). From this it follows that the actual number of stars ejected from the clusters in NGC 6357 could several times exceed the number of detected bow-shock-producing stars.

To search for bow shocks around NGC 6357, we used the archival data from the Mid-Infrared Galactic Plane Survey (Price et al. 2001), the 24 and 70 Micron Survey of the Inner Galactic Disk with MIPS[3] (MIPSGAL; Carey et al. 2009) and the preliminary data release of the Mid-Infrared All Sky Survey carried out with the Wide-field Infrared Survey Explorer (WISE; Wright et al. 2010). The first survey, carried out with the Spatial Infrared Imaging Telescope onboard the Midcourse Space Experiment (MSX) satellite, covers the entire Galactic plane within $|b| < 5°$ and provides images at 18 arcsec resolution in four mid-infrared spectral bands centred at 8.3 μm (band A), 12.1 μm (band C), 14.7 μm (band D), and 21.3 μm (band E). The MIPSGAL survey (carried out with the *Spitzer* Space Telescope) mapped 278 square degrees of the inner Galactic plane ($|b| < 1°$ is covered for $5° < l < 63°$ and $298° < l < 355°$ and $|b| < 3°$ is covered for $|l| < 5°$) and provides 24 μm images at 6 arcsec resolution. The current release of the WISE survey covers 57 per cent of the sky and provides images at four wavelengths: 3.4, 4.6, 12 and 22 μm, with angular resolution of 6.1, 6.4, 6.5 and 12.0 arcsec, respectively. The advantage of the MSX and WISE surveys is that they cover the whole Galactic plane and extend to higher Galactic latitudes than the MIPSGAL one, thereby allowing us to search for high-velocity runaways ejected at large angles to the Galactic plane (which could be off the region covered by the MIPSGAL survey). On the other hand, the better angular resolution of the MIPSGAL survey could be vital for the detection of bow shocks generated by stars moving through the dense gas of the parent molecular cloud. To search for possible optical counterparts to the bow shocks and to identify their associated stars, we used the Digitized Sky Survey II (DSS-II; McLean et al. 2000).

Assuming that the age of the star clusters in NGC 6357 is ∼1–2 Myr and adopting the typical velocity of runaway stars of ∼30–50 km s^{-1}, one finds that stars leaving the clusters at the very beginning of their dynamical evolution would be confined within ∼1−3° from NGC 6357. Thus, one can neglect the effect of the Galactic gravitational potential on their trajectories. Correspondingly, one can expect that the bow shocks produced by the ejected stars would be directed away from their parent

[3] MIPS = Multiband Imaging Photometer for *Spitzer* (Rieke et al. 2004).

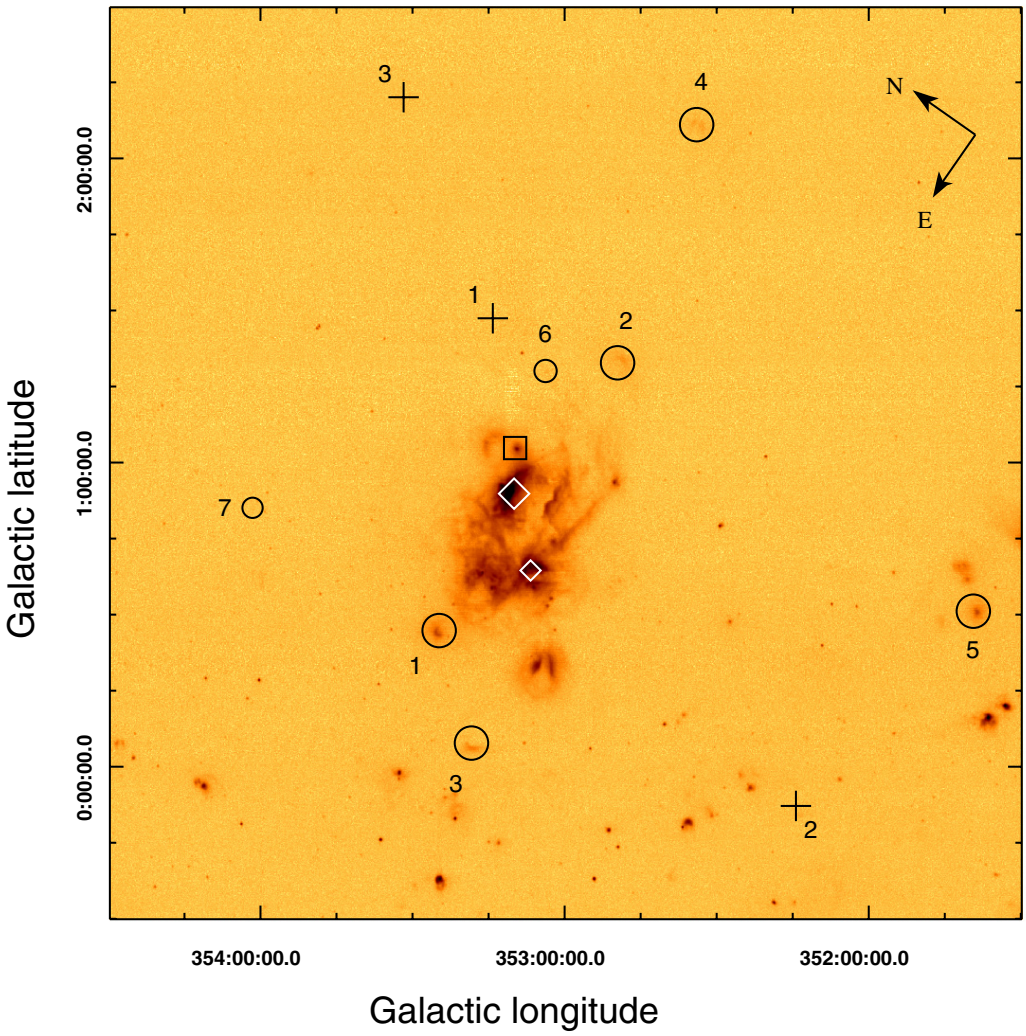

Fig. 1. 3° × 3° 21.3 μm (MSX band E) image of the H II region NGC 6357 (containing the star clusters Pismis 24 and AH03 J1725−34.4) and its environments. The positions of seven bow shocks detected with MSX and *Spitzer* are marked by large and small circles, respectively. The position of the two most massive stars in Pismis 24 (which define the centre of the cluster) is indicated by a large diamond. The position of the most massive star in the cluster AH03 J1725−34.4 is marked by a small diamond. The position of IRAS 17207−3404 is indicated by a square, while the positions of three circular shells are indicated by crosses (see text for details).

clusters, provided that there are no peculiar large-scale flows in the interstellar medium through which the stars are moving.

First, we searched for bow shocks using the MSX data. The search was carried out in a 12° wide area elongated along the Galactic plane and centred at the longitude of NGC 6357 ($l \simeq 353°$). Along the Galactic latitude, the search was limited by the MSX coverage ($|b| < 5°$), so that potentially we were able to detect bow shocks produced by stars leaving the cluster immediately after its formation and moving perpendicularly to the Galactic plane with a peculiar (tangential) velocity of ~100 km s^{-1}. The visual inspection of MSX 21.3 μm images revealed five bow shocks (indicated in Fig. 1 by large circles). All of them have a clear arc-like structure that opens towards NGC 6357 (Figs. 2–6), which suggests that these structures are generated by stars expelled from this star-forming region. Bow shock 4 has a prominent gap on its leading edge (Fig. 5; see also below). All five bow shocks are most prominent at 21.3 μm, although some of them are visible in other MSX wavebands as well. Bow shock 3 has an obvious optical counterpart in the DSS-II (see Fig. 4), while bow shocks 1 and 5 are embedded in H II regions (the H II region associated with bow shock 5 is known as GAL 351.66+00.52; Lockman 1989).

Then, we used the data from the MIPSGAL survey. Four of the bow shocks discovered with MSX were covered by this survey and we give their MIPS 24 μm images in Fig. 7. We also discovered two new bow shocks whose orientation is consistent with the possibility that their associated stars were ejected

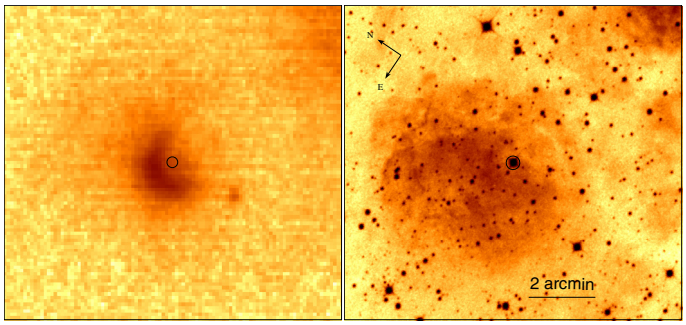

Fig. 2. *Left*: MSX 21.3 μm image of bow shock 1. *Right*: DSS-II (red band) image of the same field. The position of the bow-shock-producing star (star 1) is marked by a circle.

from NGC 6357 (see Figs. 8 and 9 and compare them with Fig. 1, where the positions of these bow shocks are indicated by small circles). The angular extent of both bow shocks (~30 arcsec) is several times smaller than that of the bow shocks discovered with MSX, which can be understood if the stars generating these two bow shocks are either moving through the denser ambient medium (e.g. the background molecular cloud) or/and have weaker winds and higher peculiar velocities. Neither of these bow shocks were detected in the optical range.

The use of the WISE data did not result in discovery of new bow shocks around NGC 6357. All seven bow shocks detected

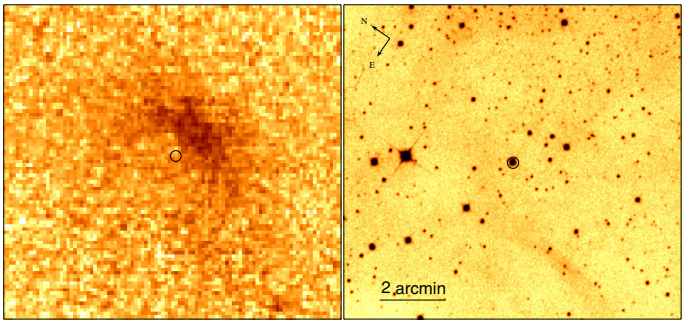

Fig. 3. *Left*: MSX 21.3 μm image of bow shock 2. *Right*: DSS-II (red band) image of the same field. The position of the bow-shock-producing star (star 2) is marked by a circle.

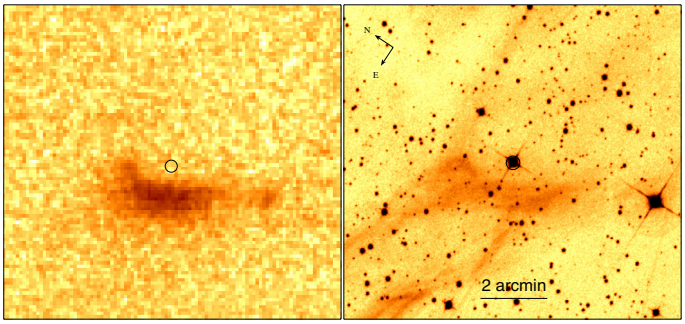

Fig. 4. *Left*: MSX 21.3 μm image of bow shock 3. *Right*: DSS-II (red band) image of the same field. The position of the bow-shock-producing star (star 3 or HD 319881) is marked by a circle.

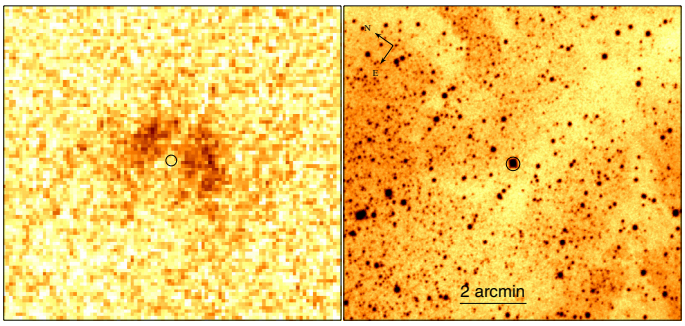

Fig. 5. *Left*: MSX 8.3 μm image of bow shock 4. *Right*: DSS-II (red band) image of the same field. The position of the bow-shock-producing star (star 4) is marked by a circle.

with *MSX* and *Spitzer* are clearly visible in the WISE data as well. In Fig. 10 we present images of bow shock 4 (not covered by the MIPSGAL survey) at all four WISE wavelenghts, showing its curious fine structure (most prominent at 12 and 22 μm). The possible origin of the gap in the leading edge of bow shock 4 and the cirrus-like filaments around it are discussed in Sect. 6.

A by-product of our search for bow shocks using the *Spitzer* data is the discovery of a compact arcuate nebula attached to one of the candidate OB stars revealed with *Chandra* (namely, star 9 from Table 7 of Wang et al. 2007). The MIPS 24 μm image of this nebula is saturated, so that we give in Fig. 11 the *Spitzer* 8, 4.5 and 3.6 μm images obtained with the Infrared Array Camera (IRAC; Fazio et al. 2004) within the Galactic Legacy Infrared Mid-Plane Survey Extraordinaire (GLIMPSE; Benjamin et al. 2003). The orientation and the small angular size of the nebula (embedded in the more extended region of infrared emission known as IRAS 17207−3404; marked in Fig. 1

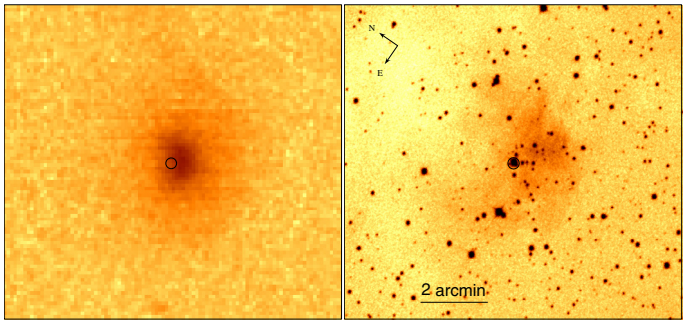

Fig. 6. *Left*: MSX 21.3 μm image of bow shock 5. *Right*: DSS-II (red band) image of the same field. The position of the bow-shock-producing star (star 5 or [N78] 34) is marked by a circle.

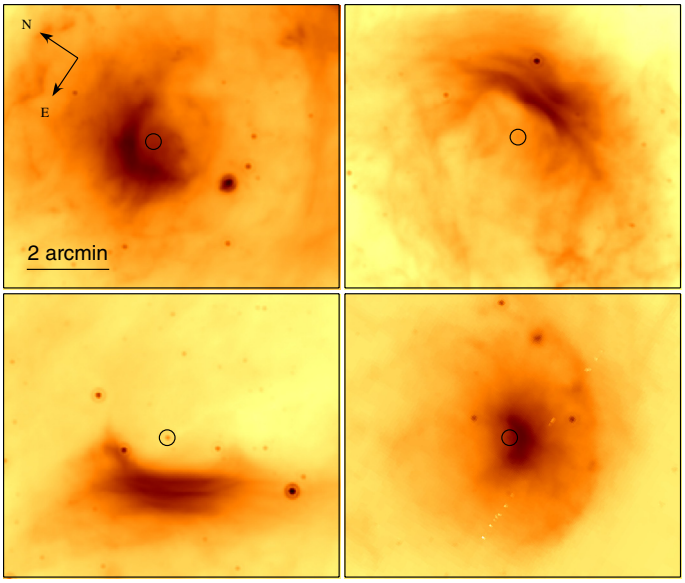

Fig. 7. From left to right, and from top to bottom: MIPS 24 μm images of bow shocks 1, 2, 3, and 5. The positions of the associated stars are marked by circles. The orientation and the scale of the images are the same.

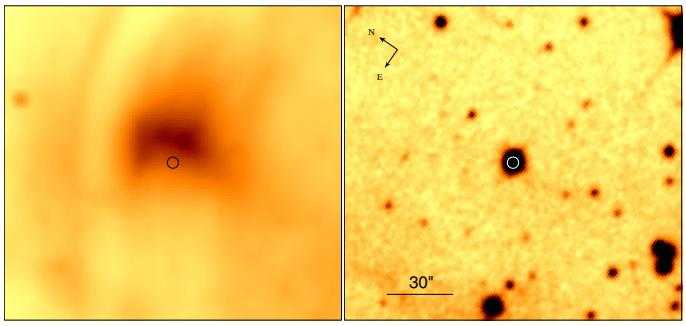

Fig. 8. *Left*: MIPS 24 μm image of bow shock 6. *Right*: DSS-II (red band) image of the same field. The position of the bow-shock-producing star (star 6) is marked by a circle.

by a square) are consistent with the interpretation of the nebula as a bow shock generated by a massive star ejected from Pismis 24 and moving through the dense background molecular cloud. Correspondingly, the extended IRAS source can be interpreted as an H II region created by the ionizing emission of the star (cf. Paper I; Gvaramadze et al. 2011b). Alternatively, the nebula could be a circumstellar (toroidal) shell, similar to those observed around some evolved massive stars (see, e.g., Fig. 4 in

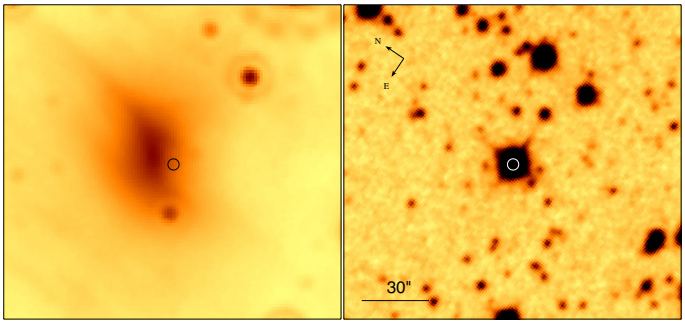

Fig. 9. *Left*: MIPS 24 μm image of bow shock 7. *Right*: DSS-II (red band) image of the same field. The position of the bow-shock-producing star (star 7) is marked by a circle.

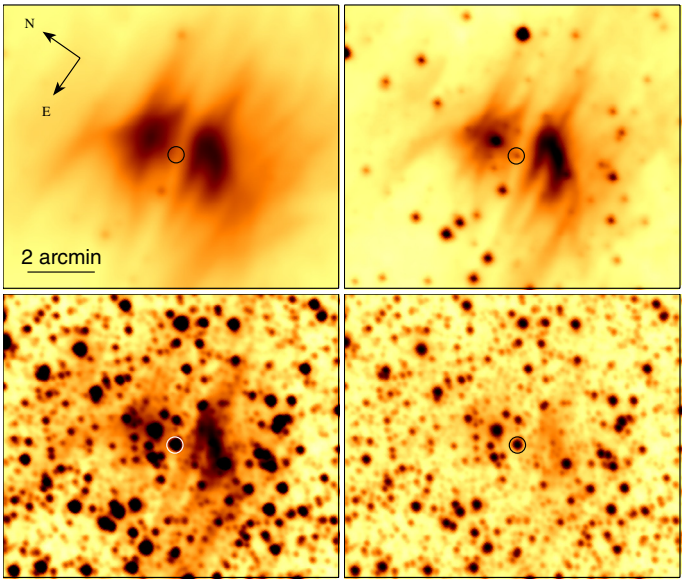

Fig. 10. From left to right, and from top to bottom: WISE 22, 12, 4.6 and 3.4 μm images of bow shock 4. The position of the associated star (star 4) is marked by a circle. The orientation and the scale of the images are the same.

Gvaramadze et al. 2010c, for the IRAC 5.8 μm image of a nebula around the candidate luminous blue variable star MN 56). The 2MASS photometry of the star, however, suggests that it could be a main-sequence late O-type star (see Sect. 4), so that we consider the bow-shock interpretation of the arcuate nebula as more preferable. Note that the candidate OB star associated with the nebula is separated from the centre of Pismis 24 by only $\simeq$9 arcmin, i.e. it is located (at least in projection) well within the cluster halo. For the sake of completeness, we give the details of this star (hereafter star 8) in Table 1.

Another by-product of the search for bow shocks with *Spitzer* is the discovery of three ring-like shells with central point sources. We present these shells and discuss their origin in Sect. 5.

4. Bow-shock-producing stars

Inspection of the DSS-II (red band) images suggested that the bow shocks discovered with MSX and *Spitzer* are associated with stars indicated in Figs. 2–9 by circles. The details of these stars are given in Table 1. Columns 2, 3, 5, and 6 give the equatorial coordinates of the stars and their J- and K_S-magnitudes (all taken from the 2MASS catalogue; Skrutskie et al. 2006), while

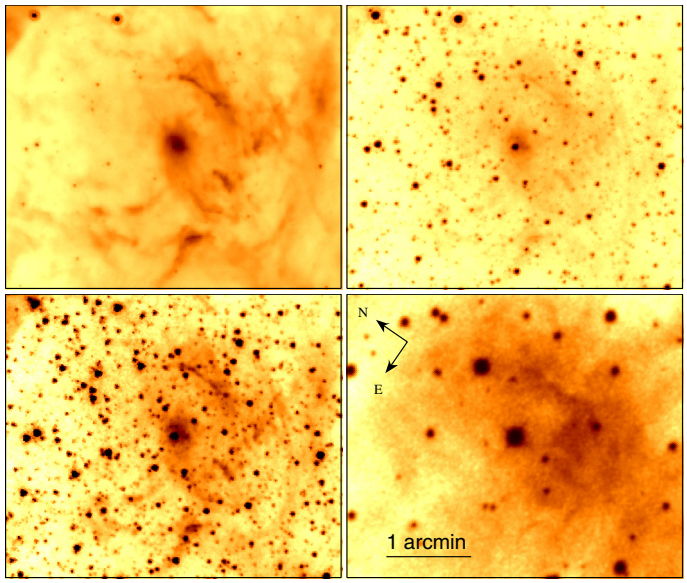

Fig. 11. From left to right, and from top to bottom: IRAC 8, 4.5 and 3.6 μm, and DSS-II (red band) images of the candidate bow-shock-producing star (star 8) embedded in the extended region of infrared emission (known as IRAS 17207−3404). The orientation and the scale of the images are the same.

Col. 4 gives the visual magnitudes of the stars taken from the NOMAD catalogue (Zacharias et al. 2004). Columns 7 and 8 give the K_S-band interstellar extinction towards the stars and their absolute magnitudes in the same band derived under the assumption that the stars are located at the same distance as NGC 6357. Column 9 provides spectroscopic and photometric (enclosed in brackets) spectral types of the stars (see below).

Using the SIMBAD database[4] and the VizieR catalogue access tool[5], we found that two of the five bow shocks discovered with MSX are generated by known OB stars (with spectroscopically derived spectral types). Namely, it turns out that bow shocks 3 and 5 are produced by the O6 Vn (Drilling & Perry 1981) star HD 319881 and the O8/B0 III/V (Neckel 1984) star [N78] 34, respectively. To determine the nature of the other three stars (hereafter stars 1, 2 and 4), we obtained their spectra with the South African Astronomical Observatory (SAAO) 1.9-m telescope (see Sect. 4.1). The stars associated with the bow shocks discovered with *Spitzer* (hereafter stars 6 and 7) still have to be observed spectroscopically. If, however, we assume that these two stars are located at the same distance as NGC 6357, then one can estimate their spectral types using the 2MASS photometry and calibration of absolute magnitudes and intrinsic colours (see Sect. 4.2).

4.1. Spectral types of the bow-shock-producing stars 1, 2 and 4

The observations of stars 1, 2 and 4 were performed with the Cassegrain spectrograph using a long slit of $3' \times 1.8''$ on 2009 June 1 and 2. Grating with 300 lines mm^{-1} was used with the 266×1798 pixels CCD detector SITe with two setups with the wavelength coverage of ~3760–7750 Å for stars 1 and 4 and ~3560–7550 Å for star 2. For both setups the spectral resolution was ~2.3 Å pixel^{-1} (*FWHM* ~ 7 Å) along the dispersion

[4] http://simbad.u-strasbg.fr/simbad/
[5] http://webviz.u-strasbg.fr/viz-bin/VizieR

Table 1. Details of seven bow-shock-producing stars (stars 1–7) and one candidate bow-shock-producing star (star 8) detected around NGC 6357.

Star	RA (2000)	Dec (2000)	V	J	K_s	A_{K_s}	M_{K_s}	Spectral type
1	17 27 11.23	−34 14 34.9	11.77	8.42	7.84	0.52	−3.84	O7.5:[a] (O7 V)
2	17 22 03.43	−34 14 24.1	13.59	8.94	8.01	0.75	−3.89	O5.5:[a] (O6.5-7 V)
3 or HD 319881	17 28 21.67	−34 32 30.3	10.14	7.54	7.10	0.43	−4.48	O6 Vn[b] (O5 V)
4	17 18 15.40	−34 00 06.1	11.80	8.19	7.53	0.57	−4.19	O6.5:[a] (O6 V)
5 or [N78] 34	17 22 05.62	−35 39 55.5	13.11	8.68	7.82	0.71	−4.04	O8/B0 III/V[c] (O6.5 V)
6	17 22 50.02	−34 03 22.4	13.90	9.68	8.81	0.71	−3.05	(B0 V)
7	17 27 12.53	−33 30 40.0	12.18	9.21	8.65	0.51	−3.01	(B0 V)
8	17 24 05.62	−34 07 09.5	11.74	9.03	8.46	0.51	−3.20	(O9-9.5 V)

Notes. The last column provides spectroscopic and photometric (enclosed in brackets) spectral types of the stars (see text for details). [(a)] This work. [(b)] Drilling & Perry (1981). [(c)] Neckel (1984).

direction and the scale along the slit was 1.″4 pixel^{-1}. The seeing during the observations varied from 1.0 to 2.1 arcsec from object to object, but was stable for each object. Exposure times were 3 × 300, 3 × 600 and 3 × 300 s for stars 1, 2 and 4, respectively. The observations of star 2 were made in variable conditions, with drastic drops in transparency, resulting in the worse quality of the resulting spectrum. Spectra of Cu–Ar comparison arcs were obtained to calibrate the wavelength scale. The spectrophotometric standard stars LTT 7379 and LTT 3864 were observed with a slit width of 5 arcsec at the beginning and at the end of the nights for flux calibration. Data reduction was performed using standard procedures (see, e.g., Kniazev et al. 2008, for details).

Figure 12 presents the resulting normalized spectra of stars 1, 2 and 4 in the $\lambda\lambda$4000–7000 Å region. All three spectra show numerous narrow absorption lines of hydrogen, He I and He II, which is typical of O-type stars. Si IV λ4089 and O III λ5592 absorptions are also visible in the spectra. We detected the emission of C III λ5696 in all three spectra (which characterizes the stars of the O4–O8 spectral type; Walborn 1980), although in the spectrum of star 2 the detection is marginal. No forbidden lines can be seen in the spectra. Numerous diffuse interstellar bands (DIBs) are present in the spectra. A blend of strong Na I λ5890, 96 absorption lines is of circumstellar or interstellar origin, while the strong absorptions visible at $\lambda > 6800$ Å are telluric in origin.

To determine the spectral types of stars 1 and 4, we used the traditional classification criteria based on the ratio of the equivalent widths (*EW*s) of H I λ4471 and He II λ4541 lines (Morgan et al. 1943; Conti & Alschuler 1971). Using Table 3 in Conti & Alschuler (1971) and *EW*s given in Table 2, we found the spectral types of stars 1 and 4 to be O7.5 and O6.5, respectively, with an uncertainty of ±1 subtype. The more earlier subtype inferred for star 4 is consistent with the increase of the C III λ5696 emission line strength with luminosity (Walborn 1980). Similarly, using Table 5 in Conti & Alschuler (1971) and *EW*s of Si IV λ4089 and He I λ4143 lines from Table 2, we found that both stars are supergiants. This inference, however, is inconclusive because of the large errors in the measurements of the Si IV λ4089 line, which allow the two stars to belong to any luminosity class (see also below).

The poor observational conditions and the relatively high extinction towards star 2 (see Table 1) degraded the spectrum of the star, which precludes us from using traditional classification criteria. Instead, we utilized the classification scheme for O stars in the yellow-green ($\lambda\lambda$4800–5420 Å) proposed by Kerton et al. (1999), which is based on the ratio of *EW*s of the lines He I λ4922 and He II λ5411:

$$\mathrm{SpT} = (9.04 \pm 0.10) + (4.10 \pm 0.23) \log EW_{4922}/EW_{5411}. \quad (3)$$

Using Eq. (3) and *EW*s given in Table 2, we found SpT ≃ 5.5. Similarly, applying this equation for stars 1 and 4 gives their spectral types of O8 and O7, respectively, which agree well with the estimates based on the traditional classification criteria. The spectral type can also be estimated using separately EW_{4922} and EW_{5411} (Kerton et al. 1999):

$$\mathrm{SpT} = (4.82 \pm 0.03) + (7.92 \pm 0.56) EW_{4922}, \quad (4)$$

$$\mathrm{SpT} = (12.80 \pm 0.41) - (7.08 \pm 0.58) EW_{5411}. \quad (5)$$

From Eqs. (4) and (5), we found SpT ≃ 6.0 and 5.0, respectively; both estimates are consistent with that derived from Eq. (3). Still, although it is clear that star 2 is of O-type, the estimates of its spectral type suffer from the large errors of measured *EW*s (see Table 2).

The lack of an exact spectral classification does not allow us to compare the spectroscopic distances to stars 1, 2 and 4 with the distance to NGC 6357. Instead, we use the assumption that these stars were ejected from NGC 6357 to constrain their spectral types and luminosity classes. Using Eq. (1) and adopting the intrinsic colour, for O stars, $(J - K_s)_0 = -0.21$ mag (Martins & Plez 2006), we calculated the K_s-band extinction, A_{K_s}, towards these stars and their absolute magnitudes M_{K_s} (see Table 1). Then using the calibration of absolute infrared magnitudes for Galactic O stars by Martins & Plez (2006), we found that all three stars should be on the main-sequence with spectral types of O7 V, O6.5–7 V, and O6 V, which agree well with those derived from spectroscopy (see Table 1, where the photometric spectral types are enclosed in brackets).

4.2. Constraining the spectral types of the other bow-shock-producing stars

Similarly, assuming that the other bow-shock-producing stars around NGC 6357 are located at the same distance as this H II region, we calculated A_{K_s} and M_{K_s} for these stars and estimated their photometric spectral types (see Table 1). For stars 3 and 5 we found spectral types of O5 V and O6.5 V, respectively. The former estimate agrees reasonably well with the spectroscopically derived spectral type, while the latter one is inconsistent with the spectral classification reported by Neckel (1984). We note, however, that the spectral types given by Neckel (1984) are systematically later than those derived from the more recent observations (Massey et al. 2001; Damke et al. 2006). For example, one of the brightest (and most massive) stars in the cluster AH03 J1725−34.4, [N78] 51, was classified by Neckel (1984) as an O9 star, while in the recent study of this cluster by

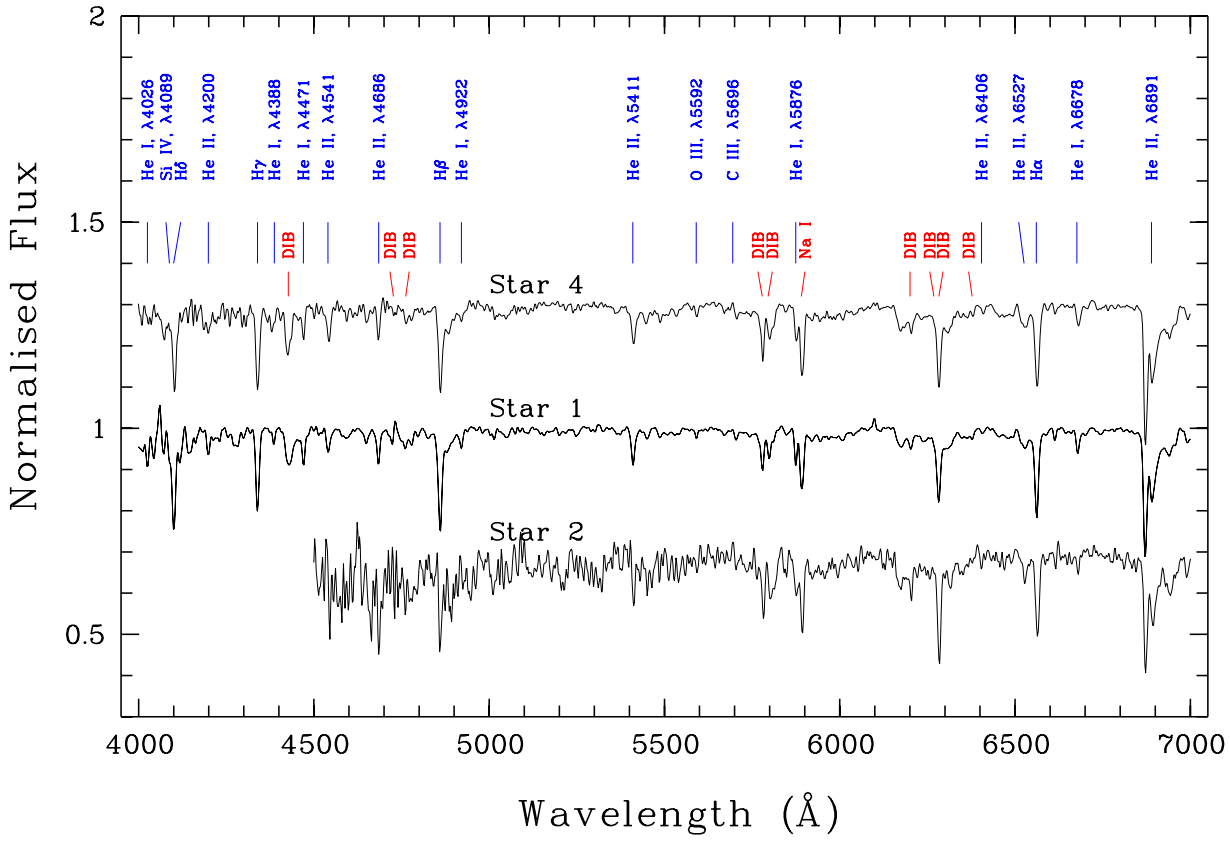

Fig. 12. Normalized spectra of stars associated with bow shocks 4 (*top*), 1 (*middle*) and 2 (*bottom*) with principal lines and most prominent DIBs indicated. The spectra of stars 4 and 2 are shifted upwards and downwards by ≃0.3 continuum flux unit, respectively.

Table 2. Equivalent widths (*EW*s; in Å) of absorption lines used for spectral classification of bow-shock-producing stars 1, 2 and 4.

Star	Si IV λ4089	He I λ4143	He I λ4471	He II λ4541	He I λ4922	He II λ5411
1	0.62 ± 0.35	0.30 ± 0.15	0.90 ± 0.12	0.75 ± 0.09	0.58 ± 0.08	1.07 ± 0.05
2	–	–	–	–	0.15 ± 0.14	1.07 ± 0.25
4	0.53 ± 0.34	0.14 ± 0.06	0.70 ± 0.12	1.00 ± 0.12	0.34 ± 0.13	1.15 ± 0.05

Damke et al. (2006) the spectral type of the star was found to be O3.5 V((f)).

Applying the same procedure for stars 6 and 7 suggests that both of them could be of the same spectral type of B0 V (so that the smaller size of the bow shocks generated by stars 6 and 7 could be because of weaker winds of these stars). And finally, we estimated the spectral type of the candidate bow-shock-producing star (star 8) to be O9–9.5 V. Additional spectroscopic and photometric observations of the bow-shock-producing stars around NGC 6357 are warranted.

4.3. Proper motions and likely parent clusters of bow-shock-producing stars

In Table 3 we provide two representative proper motion measurements for each bow-shock-producing star, found with VizieR. For most stars we used the measurements from the most recent catalogues, namely UCAC3 (Zacharias et al. 2010) and PPMXL (Röser, Demleitner & Schilbach 2010). When the UCAC3 proper motion is marked "with doubts" (because it relies on "less than two good matches"), we used the data from the NOMAD catalogue (Zacharias et al. 2004). Although most measurements are insignificant (i.e. the measurement uncertainties are comparable to the measurements themselves), it is of interest to check whether or not the orientation of the stellar peculiar velocities implied by these measurements is consistent with the distribution of the stars on the sky and with the orientation of their associated bow shocks.

To convert the observed proper motions into the transverse peculiar velocities of the stars, we used the Galactic constants R_0 = 8.0 kpc and Θ_0 = 240 km s^{-1} (Reid et al. 2009) and the solar peculiar motion $(U_\odot, V_\odot, W_\odot)$ = (10.0, 11.0, 7.2) km s^{-1} (McMillan & Binney 2010). The derived velocity components in Galactic coordinates are given in columns 5 and 6 of Table 3. For the error calculation, only the errors of the proper motion measurements were considered. Obviously, the orientation of peculiar velocities of stars 1, 2, 3, 4, 6 and 8 are consistent (within their margins of error) with the orientation of their bow shocks and with the possibility that these stars are moving away from NGC 6357. For stars 5 and 7 we found that their peculiar velocities have "wrong" orientations, i.e. are inconsistent with the orientation of the associated bow shocks.

Because of the low significance of proper motion measurements, we rely only on the orientation of the bow shocks in the identification of parent clusters for bow-shock-producing stars. We caution, however, that the close proximity of the clusters on the sky and the absence of proper motion measurements for the clusters make the identification ambiguous. Thus, the likely

Table 3. Proper-motion measurements for the seven bow-shock-producing stars (stars 1–7) and one candidate bow-shock-producing star (star 8) around NGC 6357.

Star	$\mu_\alpha \cos\delta$ mas yr^{-1}	μ_δ mas yr^{-1}	Ref.	v_l km s^{-1}	v_b km s^{-1}	Parent cluster
1	−1.5 ± 1.9	−1.6 ± 2.0	1	−4.4 ± 16.1	9.9 ± 15.3	AH03 J1725−34.4
1	−3.8 ± 3.0	−5.0 ± 3.0	2	−7.1 ± 24.2	10.0 ± 24.2	
2	−8.5 ± 4.7	−3.2 ± 4.7	3	−46.8 ± 37.9	48.5 ± 37.9	Pismis 24
2	−8.9 ± 12.2	−11.3 ± 12.2	2	−102.4 ± 98.3	14.1 ± 98.3	
3 (HD 319881)	0.0 ± 1.4	−2.8 ± 1.0	1	−5.7 ± 8.9	−5.3 ± 10.5	Pismis 24
3 (HD 319881)	3.4 ± 2.6	−3.2 ± 2.7	2	6.8 ± 21.8	−29.9 ± 21.0	
4	−4.4 ± 2.0	0.9 ± 1.1	1	−1.0 ± 11.8	39.7 ± 10.4	Pismis 24/AH03 J1725−34.4
4	−9.0 ± 2.9	2.3 ± 3.0	2	−13.2 ± 23.9	76.5 ± 23.6	
5 ([N78] 34)	−4.9 ± 4.8	11.7 ± 4.8	3	69.0 ± 38.7	93.1 ± 38.7	AH03 J1725−34.4
5 ([N78] 34)	−11.8 ± 12.2	18.7 ± 12.2	2	83.9 ± 98.3	170.9 ± 98.3	
6	−4.6 ± 3.8	0.8 ± 2.1	1	−2.5 ± 22.3	41.0 ± 27.0	AH03 J1725−34.4
6	−8.1 ± 12.2	0.1 ± 12.2	2	−23.1 ± 98.3	61.1 ± 98.3	
7	−3.9 ± 2.1	0.0 ± 1.9	1	−4.7 ± 15.8	33.1 ± 16.4	Pismis 24
7	−7.3 ± 3.0	−3.2 ± 3.0	2	−41.5 ± 24.2	41.5 ± 24.2	
8	−6.0 ± 1.8	1.9 ± 2.6	1	−1.4 ± 19.1	55.5 ± 16.8	Pismis 24
8	−9.4 ± 3.0	−2.5 ± 3.0	2	−46.2 ± 24.2	58.1 ± 24.2	

Notes. Two measurements are given for each star to indicate the uncertainties in the measurements. For each data set, the peculiar (transverse) velocities (in Galactic coordinates) were calculated and added to the table. A likely parent cluster for each star is indicated in the last column.
References. (1) UCAC3 (Zacharias et al. 2010); (2) PPMXL (Röser et al. 2010); (3) NOMAD (Zacharias et al. 2004).

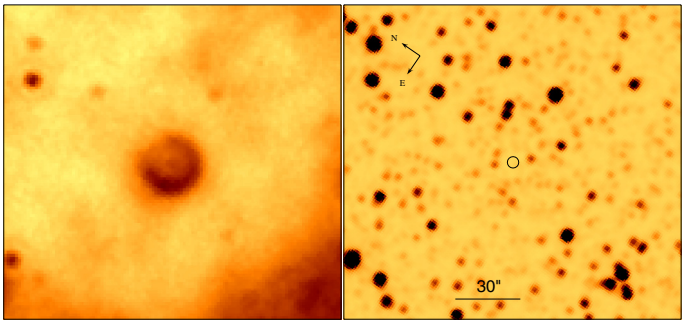

Fig. 13. *Left*: MIPS 24 μm image of shell 1. *Right*: 2MASS K_s band image of the same field with the position of the geometric centre of shell 1 indicated by a circle.

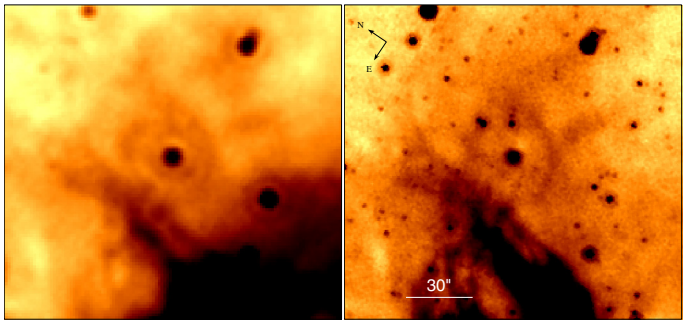

Fig. 14. *Left*: MIPS 24 μm image of shell 2. *Right*: IRAC 8 μm image of the same field.

parent clusters indicated in the last column of Table 3 should be considered as tentative.

5. Three circular shells

As we mentioned in Sect. 3, one of the by-products of the search for bow shocks around NGC 6357 with *Spitzer* is the discovery of three circular shells. The positions of these shells on the sky are marked in Fig. 1 by crosses. The appearance of all three shells (see Figs. 13–15) is typical of circumstellar shells created by luminous blue variable (LBV) stars and Wolf-Rayet stars of late WN-types (WNL) (see Gvaramadze et al. 2010c for *Spitzer* images of such shells).

One of the shells (hereafter shell 1) is located at only $\simeq 0.^{\circ}6$ (or ≃18 pc in projection) to the northwest of NGC 6357. The MIPS 24 μm image of this shell (see left panel of Fig. 13) shows a clear ring-like structure with a diameter of ≃25 arcsec and enhanced brightness along the southeast rim faced towards NGC 6357. Figure 13 also shows the central point-like source being smeared-out somewhat because of the 6 arcsec resolution of the MIPS 24 μm image. We interpret this source as a massive evolved star physically related to the shell. Many dozens of similar evolved stars were recently revealed through the detection of their infrared circumstellar shells with *Spitzer* and follow-up spectroscopy (Gvaramadze et al. 2009b, 2010a,b,c; Wachter et al. 2010, 2011). The DSS-II and 2MASS images, however, do not show any counterpart to the putative central star of shell 1. The most plausible explanation of the absence of the 2MASS counterpart is that the central star is highly absorbed by the foreground dusty material. In this connection, we note that the central stars of some circumstellar shells presented in Gvaramadze et al. (2010c) also cannot be seen in the 2MASS images, while they are visible in the IRAC (3.6, 4.5, 5.8 and 8.0 μm) ones. Unfortunately, shell 1 was not covered by the GLIMPSE survey, so that at the moment we cannot prove the existence of the central source that is apparently visible at 24 μm. Deep infrared imaging of shell 1 is therefore highly desirable. Detection of the central star and its follow-up spectroscopy would allow us to unveil the nature of the shell and potentially link the star to the star-forming region NGC 6357.

If one assumes that shell 1 is produced by a massive star ejected from NGC 6357, then the linear size of the shell is ≃0.2 pc, which is comparable to that of some LBV shells (e.g. Buemi et al. 2010). If, however, the actual size of the shell is 1–2 pc (which is more typical of circumstellar shells associated with LBV and WNL stars), then the distance to this shell is ≃7−14 kpc. At this distance the star would be at a height of ≃180−360 pc above the Galactic plane, which would imply that it is a runaway.

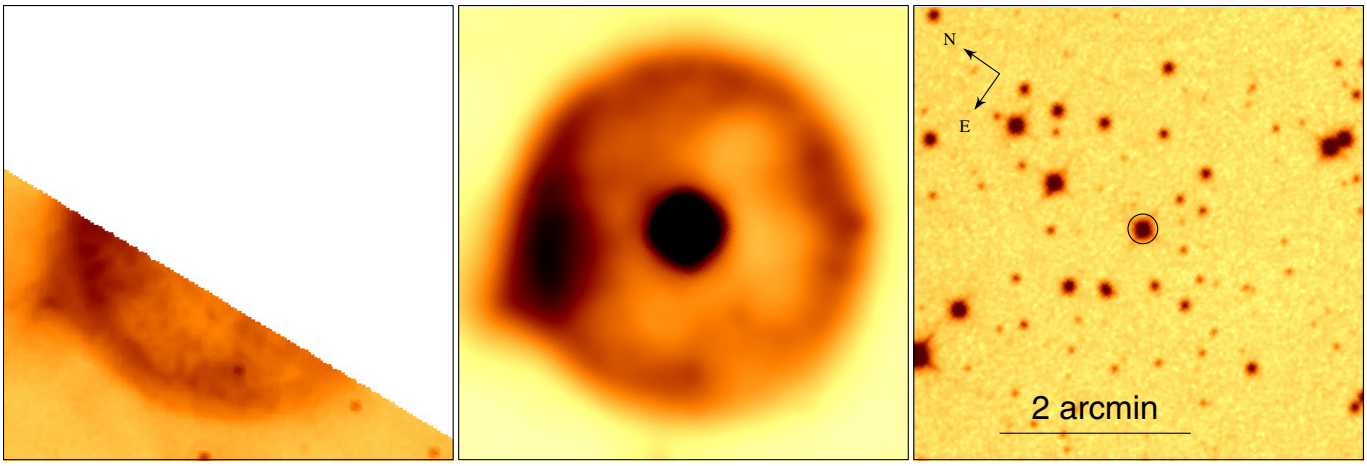

Fig. 15. *Left* and *middle*: MIPS 24 μm and WISE 22 μm images of shell 3, respectively. The MIPS image is truncated because the MIPSGAL survey covers only a part of the shell. *Right*: DSS-II (red band) image of the same field. The central star of shell 3 is marked by a circle.

Table 4. Circular shells around NGC 6357 and their central stars.

Shell	RA (2000)	Dec (2000)	V	[3.6]	[8.0]	Diameter (arcsec)
1	17 22 36.7	−33 49 10	–	–	–	25
2	17 26 19.11[a]	−35 32 37.7[a]	–	13.67[a]	8.29[a]	40
3	17 20 31.76[b]	−33 09 48.9[b]	14.3[b]	–	–	210

Notes. [(a)] GLIMPSE Source Catalog (http://irsa.ipac.caltech.edu/applications/Gator/). [(b)] NOMAD (Zacharias et al. 2004).

For the limiting K_s magnitude of the 2MASS survey of 14.8 and the K_s-band absolute magnitude of LBV and WNL stars of $\simeq$−9 and −6 mag, respectively (Blum et al. 1995; Crowther et al. 2006), one finds that $A_{K_s} \gtrsim$ 10–13 mag (or $A_V \gtrsim$ 90–110 mag) if the star is located at 1.7 kpc. An extinction this high could be understood if the star were located within (or behind) the dense molecular cloud associated with NGC 6357 (see Sect. 2).

The second shell (hereafter shell 2) is located at $\simeq$1.°3 to the south of NGC 6357. Figure 14 shows the MIPS 24 μm (right panel) and IRAC 8 μm images of this shell. The ring-like structure of shell 2 is more obvious in the 8 μm image, from which we measured a diameter of the shell of $\simeq$40 arcsec ($\simeq$0.3 pc at a distance of 1.7 kpc). The central star of shell 2 is visible not only at 24 μm, but also in all four IRAC bands. We also found a weak counterpart to this star in the 2MASS K_s-band image, which, however, is not listed in the 2MASS All-Sky Catalog of Point Sources (Skrutskie et al. 2006).

The third shell (hereafter shell 3) is located at $\simeq$1.°4 to the northwest of NGC 6357. Unfortunately, the MIPSGAL survey covers only a part of this quite extended ($\simeq$3.5 arcmin in diameter) shell with a prominent blow-up to the northeast (see left panel of Fig. 15). The full extent of shell 3, however, is visible in the WISE 22 μm image (middle panel of Fig. 15), which shows an almost circular limb-brightened nebula and its central star (visible also in the DSS-II image; right panel of Fig. 15). Using the SIMBAD database, we identified the central star with the emission-line star Hen 3-1383, classified in the literature as an Me (The 1961; Sanduleak & Stephenson 1973; Allen 1978) or a candidate symbiotic (Henize 1976) star. Our recent optical spectroscopy of Hen 3-1383 with the Southern African Large Telescope (SALT), however, showed that the spectrum of this star is almost identical to those of the prototype LBV P Cygni (see, e.g., Stahl et al. 1993) and the recently discovered candidate LBV MN 112 (Gvaramadze et al. 2010b), which implies the LBV classification for Hen 3-1383 as well (Gvaramadze et al., in prep.).

The details of the three shells are summarized in Table 4. In this table we give approximate coordinates of the geometric centre of shell 1 and the coordinates of the central stars associated with two other shells. For the central star of shell 2 we give its IRAC 3.6 and 8.0 μm magnitudes (taken from the GLIMPSE Source Catalog[6]), while for the central star of shell 3 we give its visual magnitude from the NOMAD catalogue. The last column of the table contains the angular size of the shells.

6. Discussion

We explored the idea that young star clusters lose a significant fraction of their massive stars because of gravitational few-body interactions between the cluster members. The efficiency of dynamical star ejection depends mainly on the star number density in the cluster core, which is maximum either already during cluster formation or becomes maximum later on owing to the Spitzer's mass segregation instability (Spitzer 1969). Mass segregation could be a rapid ($\lesssim$0.5 Myr) process if the cluster was born in a compact configuration (e.g. Kroupa 2008), so that dynamical star ejections could be effective well before the cluster starts to expel its members via binary-supernova explosions (the latter process becomes efficient several Myr after the formation of the first massive binary stars).

The runaway OB stars spread all around the parent cluster constitute the population of massive field stars. It is believed that most, if not all, field OB stars were formed in the clustered way (Lada & Lada 2003; Smith, Longmore & Bonnell 2009) and subsequently found themselves in the field either because of the dynamical processes in the parent clusters or because of rapid cluster dissolution (e.g., Kroupa & Boily 2002; de Wit et al. 2005; Schilbach & Röser 2008; Gvaramadze & Bomans 2008b; Pflamm-Altenburg & Kroupa 2010). Detection of massive stars in the field around young clusters and linking them to these clusters is therefore important not only for the problem of

[6] Available at http://irsa.ipac.caltech.edu/applications/Gator/.

the origin of field OB stars, but also for the problem of massive star-formation in general.

The onset of OB star ejection from a young cluster very much depends on whether the massive stars form as tight binaries near the cluster centre or not (Clarke & Pringle 1992). Thus N-body experiments can be performed with different assumptions on the OB stellar population. To see which of the theoretical (numerical) models of cluster dynamical evolution better correspond to observations, one should identify as many stars ejected from a given star cluster as possible. The detected runaway stars would constitute a sample for the future high-precise proper motion and parallax measurements with the space astrometry mission *Gaia*, which are required to determine the timing of ejections (e.g. Paper I) and thereby to constrain the initial conditions for young star clusters (Kroupa 2008) and to distinguish between the primordial and the dynamical origin of mass segregation in these clusters.

In the absence of reliable proper motion measurements for distant and/or highly obscured field OB stars, the only viable possibility to prove their runaway status and to identify their parent clusters is through the detection of bow shocks that are possibly generated by these stars[7]. The characteristic scale of bow shocks is determined (for the given number density of the ambient interstellar medium and the peculiar velocity of the star) by the strength of the stellar wind, which makes the massive stars prone for producing *detectable* bow shocks. On the other hand, the fact that dynamical star ejection is most efficient in mass-segregated clusters (Oh et al., in prep.) implies that during the early dynamical evolution of these clusters the ejected stars are preferentially the most massive ones. This inference is consistent with the observational fact that the percentage of O stars among the runaways is higher than that of B stars (e.g. Stone 1991) and could also be derived from the existence of an extended (tens of parsecs) halo of very massive (O2-type) stars around the very young (∼1–2 Myr) star cluster R136 in the Large Magellanic Cloud (e.g. Brandl et al. 2007; Walborn et al. 2002).

Our search for OB stars running away from the star-forming region NGC 6357 has resulted in the discovery of seven bow shocks. The morphology of the bow shocks suggests that the associated stars were ejected from clusters Pismis 24 and AH03 J1725−34.4, which are embedded in NGC 6357. The actual number of ejected stars could be much higher because only a small fraction of runaway stars produce observable bow shocks (see Sect. 3). Four of five (or even all; see Sect. 4.2) bow-shock-producing stars with spectroscopically determined spectral types turn out to be O-type stars, which provides additional evidence that young massive star clusters expel preferentially the most massive stars.

Follow-up spectroscopy of three bow-shock-producing stars detected around NGC 6357 showed that all of them are O-type stars. Thus, the search for bow shocks around young clusters and follow-up spectroscopy of their associated stars is a useful tool for detection of highly obscured, yet unknown OB stars. In some cases, the bow-shock-producing stars are not necessarily high-velocity runaways. For example, high-velocity outflows driven from young star clusters by the collective effect of stellar winds and ionizing emission can create bow shocks around (low-velocity; not necessarily massive) stars in the cluster's halo. In this case, the bow shocks are facing towards the cluster's centre. Numerous examples of such bow shocks were detected around young clusters and OB associations: Orion Cluster (Bally et al. 2000), Trumpler 14 (Ascenso et al. 2007), M17 and RCW 49 (Povich et al. 2008), Cyg OB2 (Kobulnicky et al. 2010). One can also imagine the situation when a slowly (∼10 km s^{-1}) moving massive star encounters a dense medium (e.g. the remainder of the parent molecular cloud) and its wind starts to interact with the ionized gas outflowing from the cloud surface towards the star with a velocity comparable to the sound speed (≃10 km s^{-1}). In the reference frame of this gas, the stellar motion is supersonic so that a bow shock is formed ahead of the (slowly) moving star. We speculate that bow shock 1 was probably generated in this way. This possibility is suggested by the small separation (≃10 pc in projection) of star 1 from its likely birth cluster AH03 J1725−34.4, which implies that the peculiar velocity of the star could be as low as 5−10 km s^{-1}, provided that it was ejected from the cluster ∼1−2 Myr ago (cf. Table 3). Moreover, the right panel of Fig. 2 shows that bow shock 1 and its associated star are located at the periphery of the H II region, from which one can infer that star 1 has met and ionized a density enhancement on its way.

Finally, we discuss the origin of the gap at the leading edge of bow shock 4 and the curious cirrus-like filaments around it. In Gvaramadze et al. (2011b), we suggested that similar cirrus-like filaments around the bow shock generated by the high-mass X-ray binary Vela X-1 (see Fig. 2 in Gvaramadze et al. 2011b) are caused by interstellar dust grains aligned with the local interstellar magnetic field and heated by the radiation of Vela X-1. This suggestion implies that bow shock 4 propagates along the local interstellar magnetic field, which affects the compression ratio of the shocked gas by making it less dense along the flanks of the bow shock (e.g. Draine & McKee 1993). The density asymmetry in turn could affect the heating of the dust grains accumulated behind the front of bow shock 4 and thereby could be responsible for its brightness asymmetry. In the absence of reliable data on parameters of bow shock 4 and its associated star we refrain from a more detailed discussion of the problem. We note, however, that similar gaps are typical of many other bow shocks. One of them (although less impressive and not at the symmetry axis of the bow shock) is shown in Fig. 16, which presents the MIPS 24 μm image (Program Id.: 30088, PI: A.Noriega-Crespo) of a bow shock produced by the BC0.7 Ia (Walborn 1972) star HD 2905. Like bow shock 4, the bow shock around HD 2905 is surrounded by cirrus-like filaments, some of which are apparently attached to the front of the bow shock near the gap. To conclude, if our suggestion on the origin of gaps is correct, then the cirrus-like filaments around bow shocks could serve as tracers of the local magnetic field, while the bow-shock-producing stars could serve as probes of the Galactic magnetic field.

7. Summary

Search for bow-shock-producing stars around the star-forming region NGC 6357 with two embedded young (∼1−2 Myr) star clusters Pismis 24 and AH03 J1725−34.4 resulted in the discovery of seven bow shocks. The geometry of the bow shocks strongly suggests that all seven associated stars were ejected from NGC 6357. Because only a small fraction of runaway stars produce detectable bow shocks, the actual number of massive stars ejected from NGC 6357 could several times exceed the number of detected bow-shock-producing stars. This inference is consistent with the theoretical expectation that young star clusters lose a significant fraction of their massive star content at

[7] The runaway status of some field OB stars can also be confirmed via measurement of their high peculiar radial velocities, but this channel for detection of runaways does not allow us to determine the star's direction of motion on the sky and therefore cannot be used to identify their birth clusters.

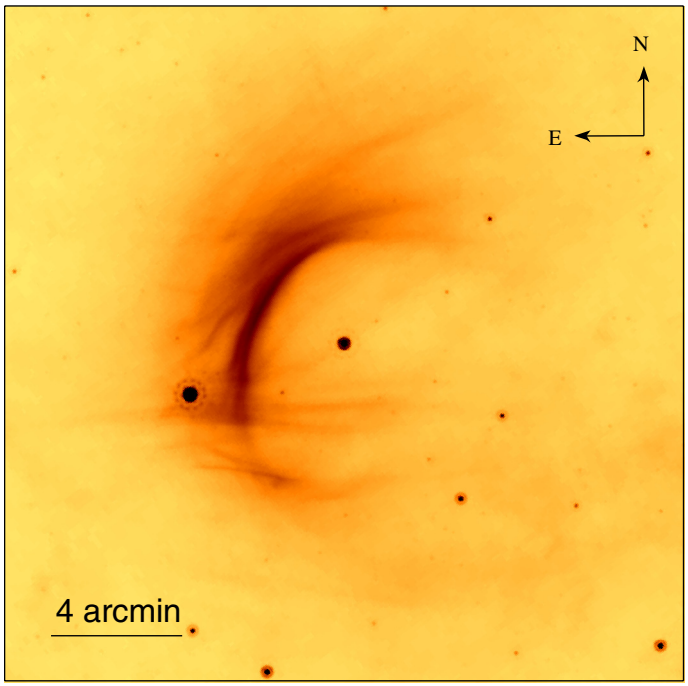

Fig. 16. MIPS 24 μm image of the bow shock generated by the BC0.7 Ia star HD 2905 and cirrus-like filaments around it (see text for details).

the very beginning of their dynamical evolution. Follow-up spectroscopy of three detected bow-shock-producing stars showed that all of them are O-type stars. This result is consistent with the observational fact that O stars prevail among the runaways and implies that search for bow shocks around massive clusters provides a useful tool for discovery of new OB stars. A by-product of our search for bow shocks is the detection of three circular shells around NGC 6357, whose morphology is typical of LBV and WNL stars. Follow-up spectroscopy of the central star of one of these shells showed that its spectrum is almost identical to that of the prototype LBV P Cygni, which implies the LBV classification for this star as well.

Acknowledgements. We are grateful to the referee for comments that allowed us to improve the presentation of the paper. V.V.G. acknowledges financial support from the Deutsche Forschungsgemeinschaft. A.Y.K. acknowledges support from the National Research Foundation of South Africa. This research has made use of the NASA/IPAC Infrared Science Archive, which is operated by the Jet Propulsion Laboratory, California Institute of Technology, under contract with the National Aeronautics and Space Administration, the SIMBAD database and the VizieR catalogue access tool, both operated at CDS, Strasbourg, France.

References

Aarseth, S. J., & Hills, J. G. 1972, A&A, 21, 255
Allen, D. A. 1978, MNRAS, 184, 601
Allison, R. J., Goodwin, S. P., Parker, R. J., et al. 2009, ApJ, 700, L99
Ascenso, J., Alves, J., Vicente, S., & Lago, M. T. V. T. 2007, A&A, 476, 199
Bally, J., ODell, C. R., & McCaughrean, M. J. 2000, AJ, 119, 2919
Baranov, V. B., Krasnobaev, K. V., & Kulikovskii, A. G. 1971, Soviet Phys. Dokl., 15, 791
Benaglia, P., Romero, G. E., Marti, J., Peri, C. S., & Araudo, A. T. 2010, A&A, 517, L10
Benjamin, R. A., Churchwell, E., Babler, B. L., et al., 2003, PASP, 115, 953
Blaauw, A. 1961, Bull. Astron. Inst. Netherlands, 15, 265
Blum, R. D., Depoy, D. L., & Sellgren, K. 1995, ApJ, 441, 603
Bohigas, J., Tapia, M., Roth, M., & Ruiz, M. T. 2004, AJ, 127, 2826
Brandl, B. R., Portegies Zwart, S. F., Moffat, A. F. J., & Chernoff, D. F. 2007, in Massive Stars in Interactive Binaries, ed. N. St.-Louis, & A. F. J. Moffat (San Francisco: ASP), 629
Brown, D., & Bomans, D. J. 2005, A&A, 439, 183
Buemi, C. S., Umana, G., Trigilio, C., Leto, P., & Hora, J. L., 2010, ApJ, 721, 1404
Cappa, C. E., Barbá, R., Duronea, N. U., et al. 2011, MNRAS, 415, 2844
Carey, S. J., Noriega-Crespo, A., Mizuno, D. R., et al. 2009, PASP, 121, 76
Clarke, C. J., & Bonnell, I. A. 2008, MNRAS, 388, 1171
Clarke, C. J., & Pringle, J. E. 1992, MNRAS, 255, 423
Conti, P. S., & Alschuler, W. R., 1971, ApJ, 170, 325
Crowther, P. A., Hadfield, L. J., Clark, J. S., Negueruela, I., & Vacca, W. D. 2006, MNRAS, 372, 1407
Damke, G., Barba, R., & Morrell, N. I. 2006, RMxAC, 26, 180
de Wit, W. J., Testi, L., Palla, F., & Zinnecker, H. 2005, A&A, 437, 247
Dias, W. S., Alessi, B. S., Moitinho, A., & Lépine, J. R. D. 2002, A&A, 389, 871
Draine, B. T., & McKee, C. F. 1993, ARA&A, 31, 373
Drilling, J. S., & Perry, C. L. 1981, A&AS, 45, 439
Evans, C. J., Walborn, N. R., Crowther, P. A., et al. 2010, ApJ, 715, L74
Fazio, G. G., Hora, J. L., Allen, L. E., et al. 2004, ApJS, 154, 10
Felli, M., Persi, P., Roth, M., et al. 1990, A&A, 232, 477
Gies, D. R. 1987, ApJS, 64, 545
Gürkan, M. A., Freitag, M., & Rasio, F. A. 2004, ApJ, 604, 632
Gvaramadze, V. V. 2007, A&A, 470, L9
Gvaramadze, V. V., & Bomans, D. J., 2008a, A&A, 485, L29
Gvaramadze, V. V., & Bomans, D. J., 2008b, A&A, 490, 1071 (Paper I)
Gvaramadze, V. V., & Gualandris, A. 2011, MNRAS, 410, 304
Gvaramadze, V. V., Gualandris, A., & Portegies Zwart, S. 2009a, MNRAS, 396, 570
Gvaramadze, V. V., Fabrika, S., Hamann, W.-R., et al. 2009b, MNRAS, 400, 524
Gvaramadze, V. V., Kniazev, A. Y., Hamann, W.-R., et al. 2010a, MNRAS, 403, 760
Gvaramadze, V. V., Kniazev, A. Y., Fabrika, S., et al. 2010b, MNRAS, 405, 520
Gvaramadze, V. V., Kniazev, A. Y., & Fabrika, S. 2010c, MNRAS, 405, 1047
Gvaramadze, V. V., Kroupa, P., & Pflamm-Altenburg, J. 2010d, A&A, 519, A33
Gvaramadze, V. V., Pflamm-Altenburg, J., & Kroupa, P. 2011a, A&A, 525, A17
Gvaramadze, V. V., Röser, S., Scholz, R.-D., & Schilbach, E. 2011b, A&A, 529, A14
Henize, K. G. 1976, ApJS, 30, 491
Huthoff, F., & Kaper, L. 2002, A&A, 383, 999
Kaper, L., Comerón, F., & Barziv, O. 1999, in Wolf-Rayet Phenomena in Massive Stars and Starburst Galaxies, ed. K. A. van der Hucht, G. Koenigsberger, & P. R. J. Eenens (San Francisco: ASP), IAU Symp., 193, 316
Kaper, L., van Loon, J.Th., Augusteijn, T., et al. 1997, ApJ, 475, L37
Kerton, C. R., Ballantyne, D. R., & Martin, P. G., 1999, AJ, 117, 2485
Kniazev, A. Y., Zijlstra, A. A., Grebel, E. K., et al. 2008, MNRAS, 388, 1667
Kobulnicky, H. A., Gilbert, I. J., & Kiminki, D. C. 2010, ApJ, 710, 549
Kroupa, P. 2001, MNRAS, 322, 231
Kroupa, P. 2004, New Astron. Rev., 48, 47
Kroupa, P. 2008, in The Cambridge N-Body Lectures, ed. S. J. Arseth, C. A. Tout, R. A. Mardling, Lect. Not. Phys., 760 (Berlin: Springer), 181
Kroupa, P., & Boily, C. M. 2002, MNRAS, 336, 1188
Lada, C. J., & Lada, E. A. 2003, ARA&A, 41, 57
Leonard, P. J. T., & Duncan, M. J. 1990, AJ, 99, 608
Lockman, F. J., 1989, ApJS, 71, 469
Lortet, M. C., Testor, G., & Niemela, V. 1984, A&A, 140, 24
Maíz Apellániz, J., Walborn, N. R., Morrell, N. I., Niemela, V. S., & Nelan, E. P. 2007, ApJ, 660, 1480
Martins, F., & Plez, B. 2006, A&A, 457, 637
Massi, F., Brand, J., & Felli, M. 1997, A&A, 320, 972
Massey, P., DeGioia-Eastwood, K., & Waterhouse, E. 2001, AJ, 121, 1050
Massey, P., Puls, J., Pauldrach, A. W. A., et al. 2005, ApJ, 627, 477
McLean, B. J., Greene, G. R., Lattanzi, M. G., & Pirenne, B. 2000, in Astronomical Data Analysis Software and Systems IX, ed. N. Manset, C. Veillet, & D. Crabtree, ASP Conf. Ser., 216, 145
McMillan, P. J., & Binney, J. J. 2010, MNRAS, 402, 934
Mdzinarishvili, T. G., & Chargeishvili, K. B. 2005, A&A, 431, L1
Melena, N. W., Massey, P., Morrell, N. I., & Zangari, A. M. 2008, AJ, 135, 878
Moeckel, N., & Bate, M. R., 2010, MNRAS, 404, 721
Moffat, A. F. J., & Vogt, N. 1973, A&AS, 10, 135
Moffat, A. F. J., Marchenko, S. V., Seggewiss, W., et al. 1998, A&A, 331, 949
Morgan, W. W., Keenan, P. C., & Kellman, E. 1943, An Atlas of Stellar Spectra, with an Outline of Spectral Classification (Chicago: The University of Chicago Press)
Murray, S. D., & Lin, D. N. C. 1996, ApJ, 467, 728
Neckel, T. 1978, A&A, 69, 51
Neckel, T. 1984, A&A, 137, 58
Neckel, T., & Chini, R. 1981, A&AS, 45, 451
Persi, P., & Tapia, M., 2008, in Handbook of Star Forming Regions, Vol. II: The Southern Sky, ed. B.Reipurth (San Francisco: ASP), ASP Mon. Publ., 5, 456

Pflamm-Altenburg, J., & Kroupa, P. 2006, MNRAS, 373, 295
Pflamm-Altenburg, J., & Kroupa, P. 2010, MNRAS, 404, 1564
Pismis, P. 1959, Bol. Obs. Tonantzintla Tacubaya, 2, 37
Portegies Zwart, S. F., Makino, J., McMillan, S. L. W., & Hut, P. 1999, A&A, 348, 117
Poveda, A., Ruiz, J., & Allen, C. 1967, Bol. Obs. Tonantzintla Tacubaya, 4, 86
Povich, M. S., Benjamin, R. A., Whitney, B. A., et al. 2008, ApJ, 689, 242
Price, S. D., Egan, M. P., Carey, S. J., Mizuno, D. R., & Kuchar, T. A. 2001, AJ, 121, 2819
Reid, M. J., Menten, K. M., Zheng, X. W., Brunthaler, A., & Xu, Y. 2009, ApJ, 705, 1548
Rieke, G. H., & Lebofsky, M. J. 1985, ApJ, 288, 618
Rieke, G. H., Young, E. T., Engelbracht, C. W., et al. 2004, ApJS, 154, 25
Rochau, B., Brandner, W., Stolte, A., et al. 2010, ApJ, 716, L90
Röser, S., Demleitner, M., & Schilbach, E. 2010, AJ, 139, 2440
Russeil, D., Zavagno, A., Motte, F., et al. 2010, A&A, 515, A55
Sanduleak, N., & Stephenson, C. B. 1973, ApJ, 185, 899
Schilbach, E., & Röser, S. 2008, A&A, 489, 105
Schraml, J., & Mezger, P. G. 1969, ApJ, 156, 269
Skrutskie, M. F., Cutri, R. M., Stiening, R., et al. 2006, AJ, 131, 1163
Smith, R. J., Longmore, S., & Bonnell, I. 2009, MNRAS, 400, 1775
Spitzer, L., Jr, 1969, ApJ, 158, L139
Stahl, O., Mandel, H., Wolf, B., et al. 1993, A&AS, 99, 167
Stone, R. C. 1991, AJ, 102, 333
Tapia, M., Roth, M., Marraco, H., & Ruiz, M. T. 1988, MNRAS, 232, 661
Tetzlaff, N., Neuhäuser, R., & Hohle, M. M. 2011, MNRAS, 410, 190
The, P.-S. 1961, Contr. from the Bosscha Observ. Lembang., 10, 1
van Buren, D. 1993, in Massive Stars: Their Lives in the Interstellar Medium, ed. J. P. Cassinelli, & E. B. Churchwell, ASP Conf. Ser., 35, 315
van Buren, D., & McCray, R. 1988, ApJ, 329, L93
van Buren, D., Noriega-Crespo, A., & Dgani, R. 1995, AJ, 110, 2914
van der Hucht, K. A. 2001, New Astron. Rev., 45, 135
Wachter, S., Mauerhan, J. C., Van Dyk, S. D., et al. 2010, AJ, 139, 2330
Wachter, S., Mauerhan, J., van Dyk, S., Hoard, D. W., & Morris, P. 2011, Bull. Soc. Roy. Sci. Liège, 80, 291
Walborn, N. R. 1972, AJ, 77, 312
Walborn, N. R. 1980, ApJS, 44, 535
Walborn, N. R., Howarth, I. D., Lennon, D. J., et al. 2002, AJ, 123, 2754
Wang, J., Townsley, L. K., Feigelson, E. D., et al. 2007, ApJS, 168, 100
Weaver, R., McCray, R., Castor, J., Shapiro, P., & Moore, R. 1977, ApJ, 218, 377
Wright, E. L., Eisenhardt, P. R. M., Mainzer, A. K., et al. 2010, AJ, 140, 1868
Zacharias, N., Monet, D. G., Levine, S. E., et al. 2004, A&AS, 205, 4815
Zacharias, N., Finch, C., Girard, T., et al. 2010, AJ, 139, 2184